JUNE 1979 LRP 155/79

NONLINEAR MODE COUPLING AND SATURATION OF DECAY INSTABILITY IN ION BEAM - PLASMA SYSTEM

T. Honzawa, Ch. Hollenstein, Y. Kawai[+], and J. Vaclavik

[+]Research Institute for Applied Mechanics
Kyushu University, Fukuoka 812, Japan

Centre de Recherches en Physique des Plasmas
Association Confédération Suisse - Euratom
ECOLE POLYTECHNIQUE FEDERALE DE LAUSANNE

NONLINEAR MODE COUPLING AND SATURATION OF DECAY INSTABILITY IN ION BEAM - PLASMA SYSTEM

T. Honzawa, Ch. Hollenstein, Y. Kawai[+] and J. Vaclavik

+ Research Institute for Applied Mechanics, Kyushu University, Fukuoka 812, Japan

Abstract

Properties of the nonlinear mode coupling for the decay instability of the fast ion beam mode are experimentally clarified. Results are qualitatively explained by theory on the parametric excitation. Further, the nonlinear damping of the instability due to the excitation of a new subharmonic wave by mixing with the pump is observed to seriously affect its saturation.

Instabilities induced by nonlinear mode coupling in linearly stable plasma systems have been intensively studied by many workers.[1] Parametric excitation corresponds to a basic process in nonlinear mode coupling.[2] Recent experiment[3] describes the possible occurrence of the decay instability of an ion beam mode. However, details of the nonlinear mode coupling and the saturation mechanism of the instability have not yet been clarified. In this paper, we report experimental results on the problems of the decay instability of the fast ion beam mode and show that results can be qualitatively explained by theory.[2]

Here, the ion beam-plasma system was synthesized using a double plasma device with multipole magnet.[4] Density of the plasmas used here was $N_e \sim 10^9$ cm^{-3}, electron temperature $T_e \sim 1$ eV, ion temperature $T_i \sim 0.2$ eV and argon gas pressure $P \lesssim 2 \times 10^{-4}$ Torr. Keeping the potential of the "target" plasma at the ground and applying a positive potential to the "driver", beam ions could flow into the target plasma from the driver. Beam velocity v_b and density ratio $\alpha = N_b/N_i$, where N_b and N_i are densities of beam and background ions respectively, could be easily controlled. Most of measurements, however, were made with $v_b \sim C_s$ (ion acoustic velocity). Observation of the spatial evolution of the ion energy distribution[5] showed that v_b did not appreciably change its initial value over a long distance x from the grid. From data of linear wave propagation the effective temperature of the beam T_b was estimated to be about 0.1 eV.

To pump the beam-plasma system, a sinusoidal rf voltage at frequency ω was applied through a capacitor to the driver. The output signal of the signal generator had almost only the fundamental oscillation, but due to plasma nonlinearities harmonic oscillations at $n\omega$, where n is an integer, were generated within the driver plasma. Each of these harmonics, if its power is large enough, may also act as a pump, whereby the beam intensity is modulated. Measurements of patterns of waves excited in the system were made by means of an interferometric technique with a cross correlator.[6] Using a small pump power, we could excite only a small amplitude wave ($\delta N/N \simeq 0.005$) in the system, except near the grid, over a wide range of frequencies. Dispersion relation and damping rate of such a linear wave are given in Figs.1(a) and (b), where results of computation, based on a linear theory,[7] are also

presented. From these results the observed mode is found to correspond to the "fast" beam mode. As computation shows, we could observe the ion acoustic mode only near the grid because of its short damping length, which is known from Fig.1(b) by considering its shorter wavelength. Dispersion relation for large amplitude pump and subharmonic waves, as will be described below, was also obtained by means of the same technique and is shown in Fig. 1(a). The relation proves that these large amplitude waves also belong to the "fast" beam mode.[8]

As the pump power was increased, subharmonic waves were observed to be nonlinearly excited at pump powers above threshold. Measurements of wave patterns of the pump and subharmonics were made with a cross correlator. In this case a very narrow-band signal at a desired frequency, which was filtered after received by a fixed probe, was adopted as reference signal. Results show that, though the pump wave at ω always spatially damps, the subharmonic wave at $\omega/2$ rapidly grows at the beginning and then damps after its amplitude is saturated. (see Fig.2(a)) Here, we can see that the pump wave damping becomes abruptly stronger when the subharmonic appears. Further, it is found from Fig.2(b) that the point, at which the subharmonic at $\omega/2$ starts to appear, approaches the excitation plane (x = 0) with increasing pump power and the damping of the subharmonic, observed after saturation, also becomes stronger with increasing pump power. Consequently the saturation level does not change appreciably with increasing pump power. Many subharmonics at frequencies higher than $\omega/2$ were also observed at high pump powers and, for example, the subharmonic at $3\omega/2$, being the most powerful among them, was observed to have a comparable power to the one of the subharmonic at $\omega/2$. Comparison of the wave patterns of the pump at ω and the subharmonics at $\omega/2$ and $3\omega/2$ indicates that the damping lengths of these waves are related by $(X_{3/2})^{-1} \simeq (X_1)^{-1} + (X_{1/2})^{-1}$, where X_1, $X_{1/2}$ and $X_{3/2}$ are the damping lengths of the pump at ω and the subharmonics at $\omega/2$ and $3\omega/2$, respectively. This relation suggests that both the pump at ω and the subharmonic at $\omega/2$ contribute to the generation of the other subharmonic at $3\omega/2$. Threshold for the subharmonic generation at $\omega/2$ by the decay of the pump at ω was measured at various pump frequencies. The results, as shown in Fig.2(d), indicates that since the threshold value $(\delta N/N)_s$ increases nearly in proportion to ω^2, the subharmonic generation can not take place above $\omega/2\pi \simeq 700$ kHz in the present case, because there is an upper limit

in available pump power. Regardless of this, the subharmonic at $3\omega/2$ was easily observed at attainable pump powers and at $\omega/2\pi \simeq 300 \sim 600$ kHz, which correspond to frequencies of $3\omega/2\pi$ much higher than 700 kHz. These experimental results lead us to conclude that the subharmonic at $3\omega/2$ is generated not by the decay of a harmonic pump at 3ω, but by the mixing of the pump at ω and the subharmonic at $\omega/2$.

In our experiment, propagation of a test wave in a pumped system was also studied. A test wave was excited by applying a small amplitude rf voltage fed by another signal generator to the grid, and its wave pattern was measured with a cross correlator, using an attenuated signal from the generator as reference signal. With no pump a test wave was found to suffer only from the linear damping. However, when its frequency ω_t was tuned to a frequency around $\omega/2$, the test wave damping was observed to be affected by the pump. (see Fig.2(c)) At high pump powers above threshold damping may change to growth, and then the spatial growth rate, which is defined by the reciprocal of the growth length L, increases with increasing pump power, as shown in Fig.3(a), where the pump wave amplitude $\delta N/N$ versus pump power is also given. From Fig.3(a), we can roughly express the growth rate in terms of the pump wave amplitude A_1 ($\equiv \delta N/N$) and of the test wave A_t as

$$\frac{1}{L} \simeq \frac{1}{v_o A_t} \frac{\partial}{\partial t} A_t \simeq \frac{1}{v_o} \left(V A_1 - \Gamma_t \right) , \qquad (1)$$

where v_o is the phase velocity of the waves, V the mode coupling constant and Γ_t the linear damping rate of test wave. Figure 3(a) also indicates that the threshold $(\delta N/N)_t$ for a test wave to run unstable is as small as $(\delta N/N)_t \simeq 0.015$, which is a little smaller than $(\delta N/N)_s$. Moreover, the growth rate of a test wave, obtained at a given pump power and pump frequency, was found to change sensitively depending on ω_t. (see Fig.3(b)) This indicates that the growth rate has a sharp peak at $\omega_t = \omega/2$, whose half width $\Delta\omega \simeq 0.28\omega$.

The preceding results reveal the occurrence of the instability due to the parametric decay of a linearly stable coherent wave on the fast ion beam branch. In the present case, as all the pump and its daughter waves belong to the fast beam mode and have almost the same velocity, the mode coupling between the waves is essentially the same as the one in the case of an oscil-

lator. Theory on the parametric instability of an oscillator[2] gives the frequency and growth rate of the instability and the threshold for it using the same symbols as in ref.2,

$$\mathrm{Re}\,\omega = \omega_o/2 \quad , \tag{2}$$

$$\mathrm{Im}\,\omega = -\Gamma + (1/2)\left[(\lambda Z_o/\Omega_o)^2 - \Delta^2\right]^{1/2} \tag{3}$$

and

$$Z_o > (Z_o)_c = (\Omega_o/\lambda)(4\Gamma^2 + \Delta^2)^{1/2}, \tag{4}$$

where Z_o and ω_o are the amplitude and frequency of the modulation (pump), Ω_o ($\fallingdotseq \omega_o/2$) and $\Gamma (\ll \Omega_o)$ the frequency and damping of the oscillation in the absence of the modulation, Δ the mismatch defined by $\Delta = \omega_o - 2\Omega_o$ and λ (> 0) the mode coupling constant. Under the present condition we know from Fig.1(a) that for the fast beam mode Γ/Ω_o is nearly constant over a wide range of Ω_o, that is, $\Gamma \simeq \eta\Omega_o$, where η is a constant. Substituting this into eq.(4) and assuming $\Gamma^2 \gg \Delta^2$, the threshold is expressed as

$$(Z_o)_c \simeq (2\eta/\lambda)\Omega_o^2 \quad . \tag{5}$$

Comparing these with experimental results, we find a qualitative agreement between them at three points as follows: (i) As expected from eq.(2), test wave experiment shows that the mode coupling constant V depends on the relative frequency of test wave ω_t/ω and has a sharp peak at $\omega_t = \omega/2$. Further, at high pump powers the subharmonic generation is observed to occur at $\omega/2$. (ii) Assuming $V = \lambda/2\Omega_o$ and $\Gamma^2 \gg \Delta^2$, eq.(3) has the same form as eq.(1) experimentally obtained. (iii) Observed threshold for the subharmonic generation at $\omega/2$ as shown in Fig.2(d) depends on pump frequency nearly in the same manner as eq. (5).

The subharmonic wave at $\omega/2$ generated by the decay of the pump has mostly so large amplitude that it can give rise to other nonlinear phenomena, whereby its damping rate becomes larger than the linear one. Therefore, we can say that the damping rate of the subharmonic $\Gamma_{1/2}$ includes the nonlinear part as well as the linear part. The most important cause determining the nonlinear part of $\Gamma_{1/2}$ is the excitation of a new subharmonic wave at $3\omega/2$ by mixing with the pump. With this process, the new subharmonic at $3\omega/2$ gains energy from the other two waves and its amplitude $A_{3/2}$ changes as[1]

$$\frac{\partial}{\partial t} A_{3/2} = K A_1 A_{1/2} - \Gamma_{3/2} A_{3/2} \quad , \tag{6}$$

where K is the coupling constant for the mixing and $\Gamma_{3/2}$ the linear damping rate of the new subharmonic at $3\omega/2$, whose amplitude is assumed to be small enough. From a steady state solution of eq.(6) we can derive a relation for the damping lengths such as $(X_{3/2})^{-1} \simeq (X_1)^{-1} + (X_{1/2})^{-1}$, which is the same as experimentally obtained.

In conclusion, we can experimentally show that the decay of a coherent pump wave at ω on the fast beam branch into two coherent waves at $\omega/2$ on the same branch is observable in an ion beam-plasma system with $v_b \sim C_s$. Properties of the nonlinear mode coupling for the decay instability are also clarified by using the test wave propagation technique. These results can be qualitatively explained by theory. Further, the resultant subharmonic wave at $\omega/2$ is found to cause the nonlinear excitation of a new subharmonic wave at $3\omega/2$ by mixing with the pump, which strengthens its damping.

The authors thank Prof. N. Yajima and Dr. M. Kono for helpful discussions, and Mr. P. J. Paris and Mr. M. Guyot for technical supports. One of them (T. H.) is also grateful to Prof. E. S. Weibel for permission to work at this institute.

References

1 See, for example, J. Weiland and H. Wilhelmsson, Coherent Non-Linear Interaction of Waves in Plasmas (Pergamon Press, Oxford, 1977), R. J. Davidson, Methods in Nonlinear Plasma Theory (Academic Press, New York and London, 1972).

2 K. Nishikawa and C. S. Liu, Advances in Plasma Physics, VI, p 9-11 (edited by A. Simon and W. B. Thompson, John Wiley & Sons, New York, 1976). This book also includes many reviews of theoretical works on the parametric instabilities by other authors.

3 R. J. Stern, J. F. Decker and P. M. Platzman, Phys. Rev. Lett. 32, 359 (1974).

4 R. J. Taylor, K. R. McKenzie and H. Ikezi, Rev. Sci. Instrum. 43, 1675 (1972), R. Limpaecher and K. R. McKenzie, Rev. Sci. Instrum. 44, 726 (1973).

5 This also showed that α went down rapidly at small x ($\lesssim$ 5 cm) and slowly at larger x due to the inhomogeneity of the background ion density near the grid and the reduction of the beam intensity via ion-neutral collisions.

6 M. Bitter, Ch. Hollenstein, P. J. Paris and C. Rizzo, INT. 80/77 (1977) Internal Report of Centre de Recherches en Physique des Plasmas, Lausanne.

7 H. W. Hendel, M. Yamada, S. W. Seiler and H. Ikezi, Phys. Rev. Lett. 36, 319 (1976).

8 Although data for the subharmonic wave at $3\omega/2$ are not given in Fig. 1(a), we have many results with different values of v_b showing that the subharmonic at $3\omega/2$ is also on the same branch. For example, see the wave patterns in Fig. 2(a).

Figure Captions

Fig. 1. (a) Dispersion relations for linear wave (X) and large amplitude waves including pump (Δ) and subharmonic at $\omega/2$ (O), measured at $v_b \sim C_s$. (b) Damping rate of linear wave (X), measured under the same condition. Results of computation for $v_b = 1.1\ C_s$, $\alpha = 0.15$ and $\theta = T_e/T_i = 5$ are also plotted. Damping rates of the slow beam mode are omitted, because $\omega_I/\omega_R \lesssim -2.17$ ($\theta_b = T_e/T_b = 10$) and -1.46 ($\theta_b = 15$). F: fast beam mode, S: slow beam mode and A: ion acoustic mode.

Fig. 2. (a) Wave patterns of pump waves at ω and subharmonic waves at $\omega/2$ and $3\omega/2$ at pump powers below and above threshold. They are measured at $v_b \simeq 1.4\ C_s$ and $\omega/2\pi = 500$ kHz. (b) Wave patterns of subharmonic wave at $\omega/2$ at various pump powers, observed at $v_b \simeq 1.1\ C_s$ and $\omega/2\pi = 500$ kHz. (c) Wave patterns of test wave at $\omega_t = \omega/2$ at various pump powers, measured at $v_b \simeq 1.1\ C_s$ and $\omega/2\pi = 500$kHz. Here, the pump rf amplitude V_{pp} is found to be proportional to the pump power. (d) Threshold pump wave amplitude $(\delta N/N)_s$ for the subharmonic generation versus pump frequency, measured at $v_b \simeq 1.1\ C_s$. The dotted line corresponds to $(\delta N/N)_s \propto \omega^2$.

Fig. 3. (a) Growth rate of test wave at $\omega/2$ (●) and pump wave amplitude (X) versus normalized pump power. These are measured at $v_b \simeq 1.1\ C_s$, $\alpha \simeq 0.15$ and $\omega/2\pi = 500$ kHz. (b) Normalized growth rate of test wave versus frequency ω_t, measured at $v_b \simeq 1.2\ C_s$, $\omega/2\pi = 500$kHz and pump wave amplitude $\delta N/N \simeq 0.05$.

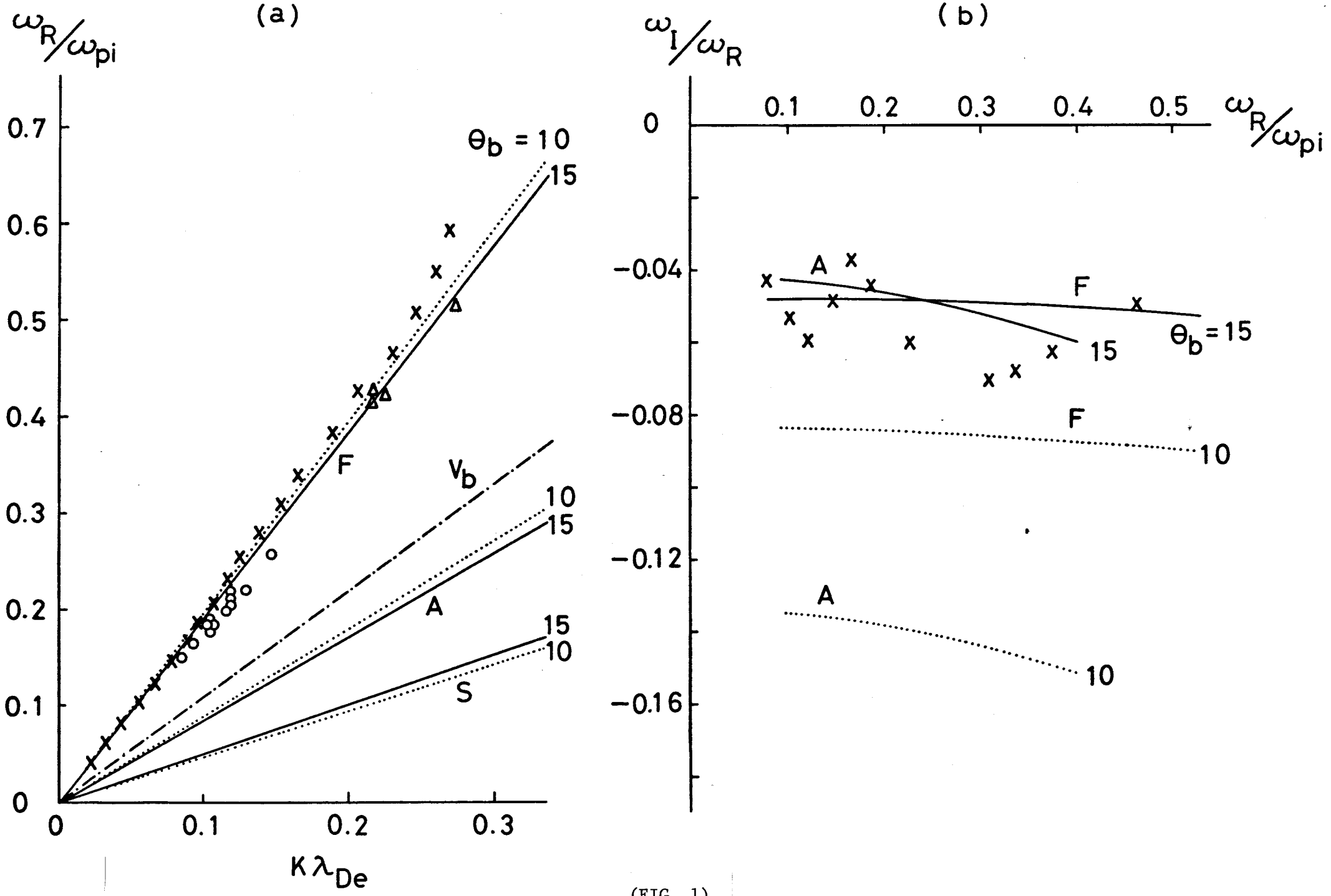
(a)
ω_R/ω_{pi}
0.7
0.6
0.5
0.4
0.3
0.2
0.1
0
$\theta_b = 10$
15
F
V_b
10
15
A
15
10
S
0
0.1
0.2
0.3
$K\lambda_{De}$
(b)
ω_I/ω_R
0
−0.04
−0.08
−0.12
−0.16
0.1
0.2
0.3
0.4
0.5
ω_R/ω_{pi}
A
F
15
$\theta_b = 15$
F
10
A
10

(FIG. 1)

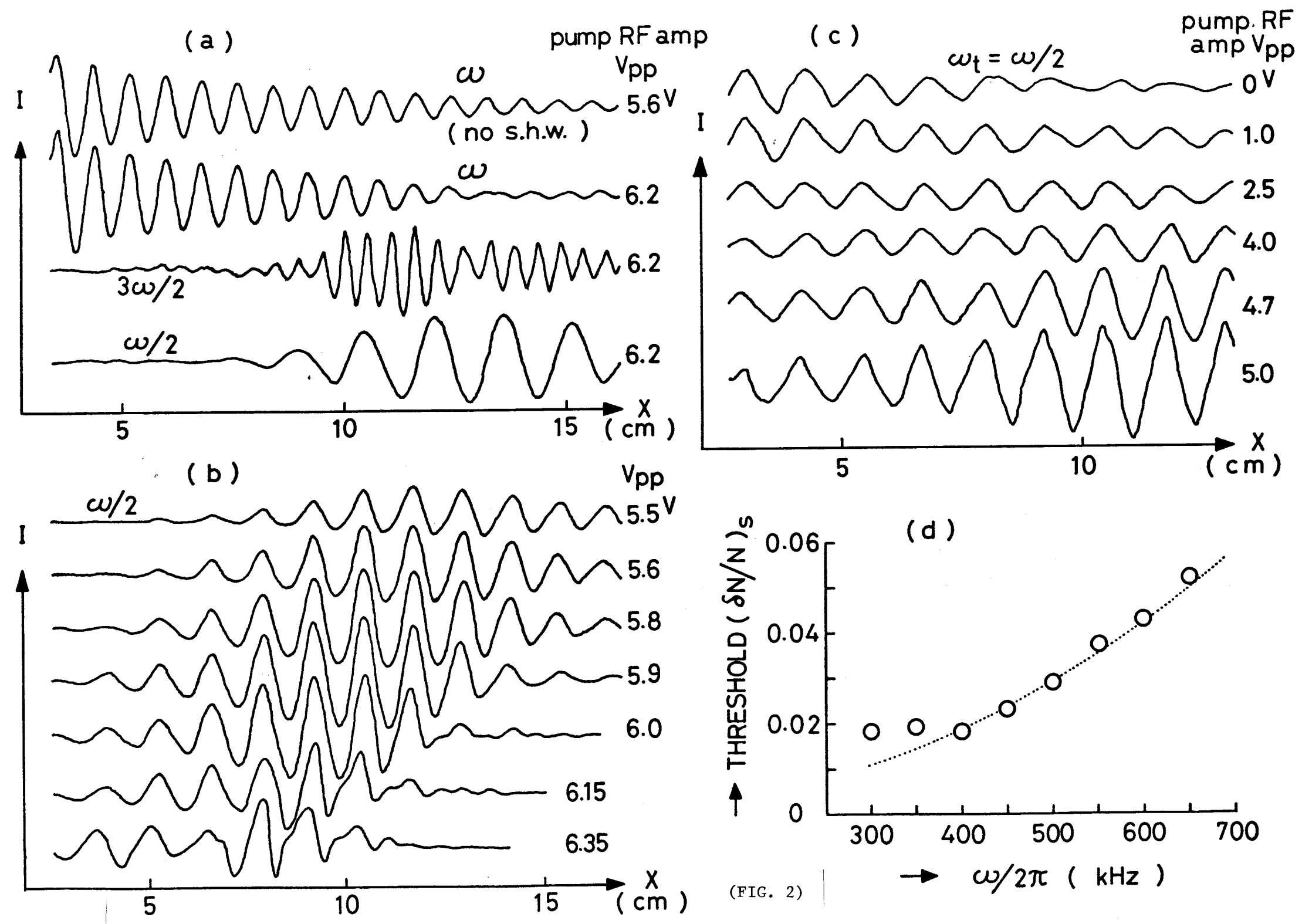
(a)
pump RF amp
Vpp
ω
5.6V
(no s.h.w.)
ω
6.2
3ω/2
6.2
ω/2
6.2
I
X
5
10
15
(cm)
(b)
Vpp
ω/2
5.5V
5.6
5.8
5.9
6.0
6.15
6.35
I
X
5
10
15
(cm)
(c)
pump. RF
amp Vpp
ωt = ω/2
0V
1.0
2.5
4.0
4.7
5.0
I
X
5
10
(cm)
(d)
THRESHOLD (δN/N)s
0.06
0.04
0.02
0
300
400
500
600
700
ω/2π (kHz)

(FIG. 2)

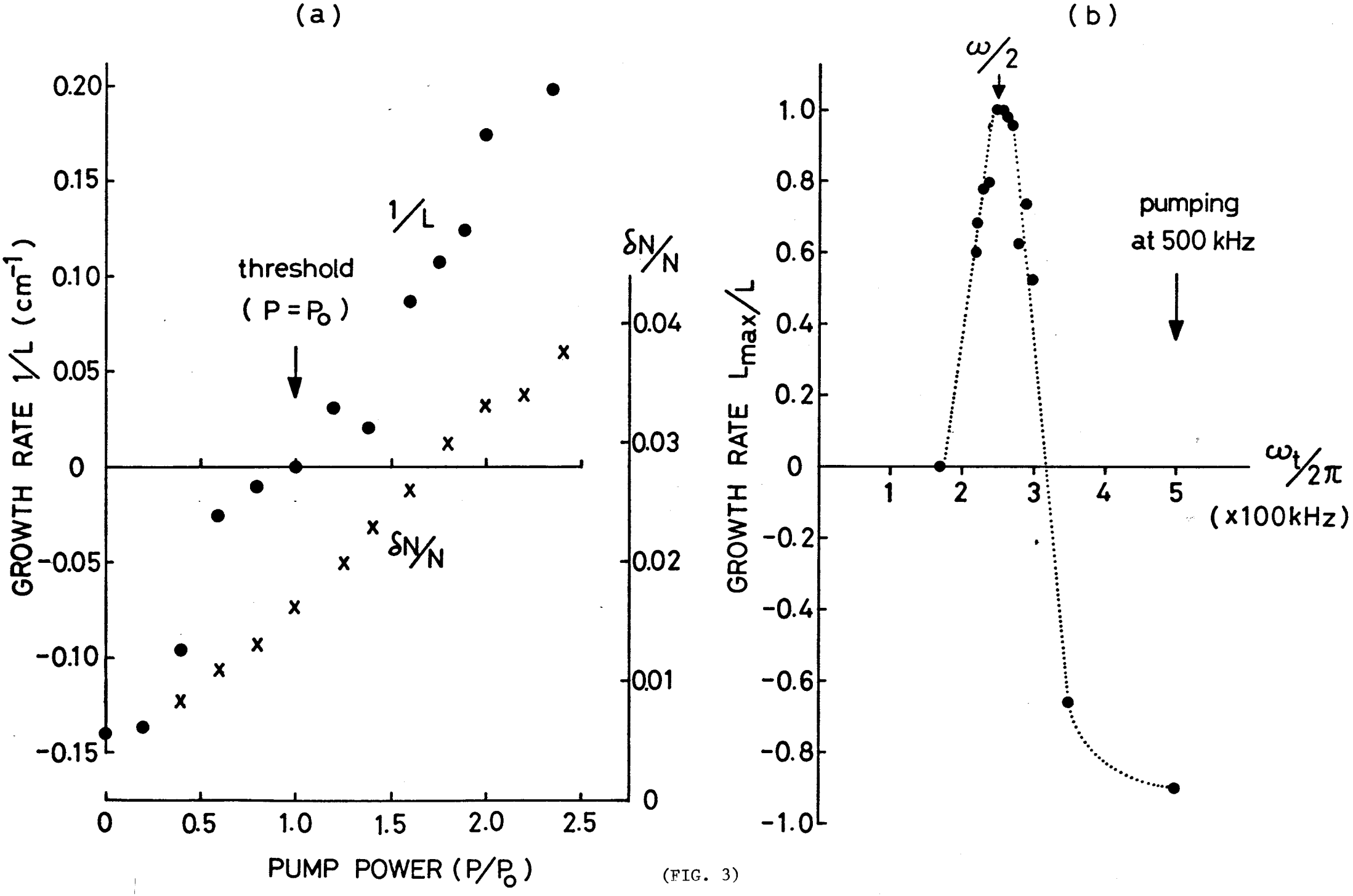
(a)
(b)
GROWTH RATE 1/L (cm⁻¹)
1/L
δN/N
threshold
(P = P₀)
PUMP POWER (P/P₀)
0.20
0.15
0.10
0.05
0
-0.05
-0.10
-0.15
0.04
0.03
0.02
0.01
0
0.5
1.0
1.5
2.0
2.5
GROWTH RATE Lmax/L
ω/2
pumping
at 500 kHz
ω_t/2π
(x100kHz)
1.0
0.8
0.6
0.4
0.2
-0.2
-0.4
-0.6
-0.8
-1.0
1
2
3
4
5

(FIG. 3)